SP-333-1

A Numerical Analysis Methodology for the Strengthening of Deep Cap Beams

Rafael A. Salgado, Serhan Guner

Synopsis: A significant number of in-service bridges have been subjected to loads above their original design capacities due to the increase in traffic and transported freight in the past decades. Externally bonded fiber reinforced polymers (FRP) is a non-destructive retrofit technique that has become common for the strengthening of overloaded cap beams of bridges. However, there is a lack of analysis methods for the retrofitted cap beams that can accurately predict the retrofitted structural response while accounting for the critical material behaviors such as bond-slip relationships, confinement effects, and redistribution of stresses. In this study, an analysis methodology using nonlinear finite element models is proposed for cap beams retrofitted with externally bonded FRP fabrics. A two-stage verification of the proposed methodology was employed: a constitutive modeling and critical behavior of materials verification using experimental results available in the literature; and a system-level load capacity determination using a large, in-situ structure. The proposed methodology was able to capture the FRP-concrete composite structural behavior and the experimentally observed failure modes. The FRP retrofit layout created using the results of this study increased the capacity of the initially overloaded cap beam in 27%, granting it a 6% extra capacity under its ultimate loading condition.

Keywords*:* deep beams; nonlinear analysis; cap beam; structural assessment; FRP; retrofit; analysis methodology

ACI member **Rafael A. Salgado** is a Ph.D. student at the University of Toledo. He received his BSCE degree in 2015 from the Universidade Federal do Espírito Santo (Brazil). His research interests include finite element analysis, including nonlinear and dynamic analyses of structures.

ACI member **Serhan Guner** is an Assistant Professor in the Department of Civil Engineering at the University of Toledo, Toledo, OH. He received his Ph.D. from the University of Toronto, Toronto, ON, Canada. He is a member of Joint ACI-ASCE Committee 447, Finite Element Analysis of Reinforced Concrete Structures. His research interests include finite element modeling of reinforced concrete structures, shear effects in concrete, development of analysis software, and structural response to impact, blast, and seismic loads.

INTRODUCTION

Externally bonded fiber reinforced polymer (FRP) is a non-destructive and efficient retrofit technique that has been increasingly common for the strengthening of overloaded bridge cap beams. Despite its large applicability, there is still a lack of analytical methods for the retrofitted cap beams that can accurately predict their structural response due to the added FRP fabrics. Despite some simple equations given by codes[1,2] to obtain an estimate of the added flexural and shear capacity due to the FRP fabrics, several material behaviors that are critical to obtain an accurate response of the retrofitted structure such as bond-slip relationships, confinement effects, and redistribution of stresses are not considered. On top of that, due to their small shear spans, cap beams are usually classified as deep elements that form a direct strut action (i.e., a diagonal compressive stress field between the load application point and the supports) and do not satisfy the Euler-Bernoulli theory (i.e., plane sections remain plane). By neglecting these important structural behaviors when performing retrofit studies using FRP fabrics, the calculated FRP retrofit layout is at risk of being ineffective or even detrimental to the original cap beam. Thus, the complexity and uniqueness of each cap beam require an effective analysis approach with an accurate FRP modeling methodology to substitute any 'guess-work' with a better understanding of the structural behavior.

This study proposes an analysis methodology for deep cap beams retrofitted with externally bonded FRP fabrics. The methodology is presented in two stages with respective verifications: constitutive modeling of the critical behavior of materials; and an overall methodology application using a large, in-situ structure. The material behavior models and the modeling procedure proposed are verified using experimental results available in the literature. The overall modeling process is presented to assist in accurately analyzing cap beams using the proposed methodology.

RESEARCH SIGNIFICANCE

FRP fabrics have been commonly used to retrofit deep cap beams of in-service bridges that have become structurally deficient due to the increase in loading condition over the decades. There is a lack of holistic analysis approaches to accurately calculate the load capacity of retrofitted cap beams while accounting for the concrete's deep beam actions and the composite behavior introduced by the FRP fabrics. This study details a finite element approach that aims to provide a holistic understanding of the structural behavior and to accurately calculate the load capacity of FRP retrofitted deep cap beams.

PROPOSED CAP BEAM NUMERICAL MODELING AND SYSTEM-LEVEL ANALYSIS METHODOLOGY

A numerical modeling and system-level analysis methodology for deep cap beams retrofitted with externally bonded FRP is proposed using nonlinear finite element analysis (NLFEA). NLFEA models are suitable for the assessment of deep cap beams due to its implementation of the nonlinear effects that are characteristic of deep elements, such as the nonlinearity of the strain distribution and the effects of cracking on the stress distribution[3,4]. Using NLFEA, the performance of the structure under both the serviceability and ultimate limit state conditions can be verified and it allows for the prediction of the progression of nonlinear events (i.e., concrete cracking, reinforcement yielding, concrete crushing, and the formation of the failure mechanism). Using the proposed methodology, if the NLFEA analysis of an un-retrofitted cap beam calculates an overloaded structural state, then a retrofit study using externally bonded FRP fabrics must be conducted to ensure the adequacy of the cap beam to its ultimate loading condition. In such cases, an NLFEA analysis is essential to get an accurate capacity of the deep beam and to determine an FRP retrofit layout that effectively captures the deficiencies of the beam.

Finite element material modeling approach

The proposed approach was developed using a two-dimensional continuum finite element model. When analyzing reinforced concrete structures, proper modeling of the constitutive response and important second-order material

behaviors are crucial[5,6]. Thus, in this study, the model was developed using the computer program VecTor2[7]. Other specialized programs could also be used for this purpose; however, the selection of VecTor2 was made because it accounts for several second-order material behavior models that are particular to cracked reinforced concrete (see Table 1). VecTor2 uses a smeared rotating crack model based on the equilibrium, compatibility, and constitutive models of the Disturbed Stress Field Model[8], which is a refined version of the Modified Compression Field Theory[9] (MCFT), a theory that has been recognized and adopted by the AASHTO[10] and CSA A23.3[4] codes.

Table 1 – Material models included in VecTor2

Material behavior	Default model	Material behavior	Default model
Compression base curve	Hognestad parabola[11]	Cracking criterion	Mohr-Coulomb (Stress)[12]
Compression post-peak	Modified Park-Kent[13]	Crack width check	Max crack width of Agg/5[14]
Compression softening	Vecchio 1992-A[15]	Concrete hysteresis	Nonlinear w/plastic offsets[7]
Tension stiffening	Modified Bentz 2003[16]	Slip distortion	Walraven[17]
Tension softening	Linear[7]	Rebar hysteresis	Seckin w/Bauschinger[18]
Confinement strength	Kupfer/Richart[19,20]	Rebar dowel action	Tassios (Crack slip)[21]
Concrete dilatation	Variable - Orthotropic[19]	Rebar buckling	Refined Dhakal-Maekawa[22,23]

In the proposed methodology, the concrete is modeled using 8-degree-of-freedom quadrilateral elements (in geometrically uniform regions) or 6-degree-of-freedom triangular elements (in geometrically non-uniform regions such as inclined sections). The concrete material stress-strain response is accounted for using a plastic-offset-based nonlinear model[7]. Several pre- and post-peak models that vary in complexity and applicability are available in the literature; Table 1 summarizes the models used in this study with detailed formulation available elsewhere[7]. The concrete model includes nonlinear hysteresis rules for the unloading and reloading conditions[7] (see Figure 1a). Even though the proposed methodology includes a static pushover analysis, some parts of the cap beam will unload and some other parts will reload, as the concrete cracking and reinforcement yielding take place, thereby requiring the use of a hysteretic material behavior.

The shear reinforcement is accounted for through a smeared material model due to their even space across the element. On the other hand, the longitudinal reinforcement is modeled using discrete truss elements (1-degree-of-freedom per node) due to the large amount of steel in specific locations of the structure. The response of the reinforcing bars is modeled using a three-partite constitutive model (see Figure 1b), including a parabolic strain hardening region as per the model of Seckin[18].

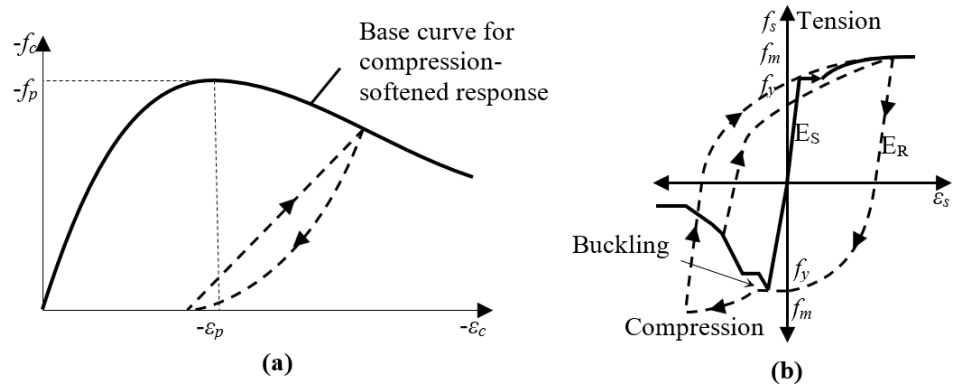

Figure 1 – (a) Concrete and (b) reinforcing steel material constitutive models.

The FRP fabrics are accounted for in the model through tension-only truss elements aligned vertically, horizontally, or in both directions depending on the fiber orientations of the fabrics. If the fabric has fibers oriented vertically, horizontally, or in both directions, the cross-sectional area of the truss elements is comprised of the effective width of each truss and the thickness of the combined FRP layers. On the other hand, if the fabric has fibers oriented in arbitrary directions, the vertical and horizontal truss-elements' sectional area are comprised of the equivalent horizontal, or vertical, fiber amount. Figures 2a and b show the case of FRP fabric with fibers oriented in an arbitrary direction, which is the most general case. The constitutive model is elastic up to their maximum tensile stress (see Figure 2c).

The modeling of the bond-slip response of the fabrics is crucial for an accurate model because it is a dominant failure mode for structures retrofitted with FRP fabrics[24]. Thus, to account for the bond-slip behavior, link elements (i.e., bi-directional springs) are used to connect the FRP truss elements to the existing concrete elements (see Figure 2d). A bi-linear constitutive model based on the fracture energy of concrete (G_f) created for the tangential bond-slip relationship between Carbon FRP (i.e., CFRP) and concrete is attributed to the link elements (see Figure 2e), with characteristic points calculated as per Equations 1-4[25,26]. For the FRP fabrics that are completely wrapped around the concrete element, perfect bonding of the fabrics nodes at the edges of the concrete element is considered (see Figure 2b). Similarly, wrapped fabrics also confine the longitudinal fabrics and provide an effective anchorage to help avoid de-bonding of the longitudinal fabrics[24,27]. Thus, the nodes of the fabrics at the anchorage regions are also perfectly bonded to the concrete. Perfect bond is modeled by specifying a high maximum bond stress for the link elements.

$$\tau_{bFy} = (54f_c')^{0.19} \leq f_r = 0.6(f_c')^{0.5} \quad (1)$$

$$G_f = \left(\tau_{bFy}/6.6\right)^2 \quad (2)$$

$$s_{Fy} = 0.057G_f^{0.5} \quad (3)$$

$$s_{Fu} = 2G_f/\tau_{bFy} \quad (4)$$

where τ_{bFy} is the maximum bond stress in MPa, f'_c is the concrete compressive strength in MPa, f_r is the modulus of rupture of the concrete in MPa, G_f is the fracture energy in N/mm, s_{Fy} is the slip at the maximum bond stress in mm, and s_{Fu} is the slip at the ultimate bond stress (i.e., zero stress) in mm.

When the FRP fabrics are wrapped around the concrete element, they provide confinement to the concrete beam. The confinement is accounted for using a smeared FRP reinforcement component in the out-of-plane direction (referred as z-direction) of the concrete elements at the edges of the beam that are wrapped by the FRP fabrics (see Figure 2b), as per Equation 5.

$$f_{c3} = -f_{sz}\rho_z \quad (5)$$

where f_{c3} is the resulting confining pressure, f_{sz} is the stress in the out-of-plane reinforcement, and ρ_z is the out-of-plane reinforcement ratio.

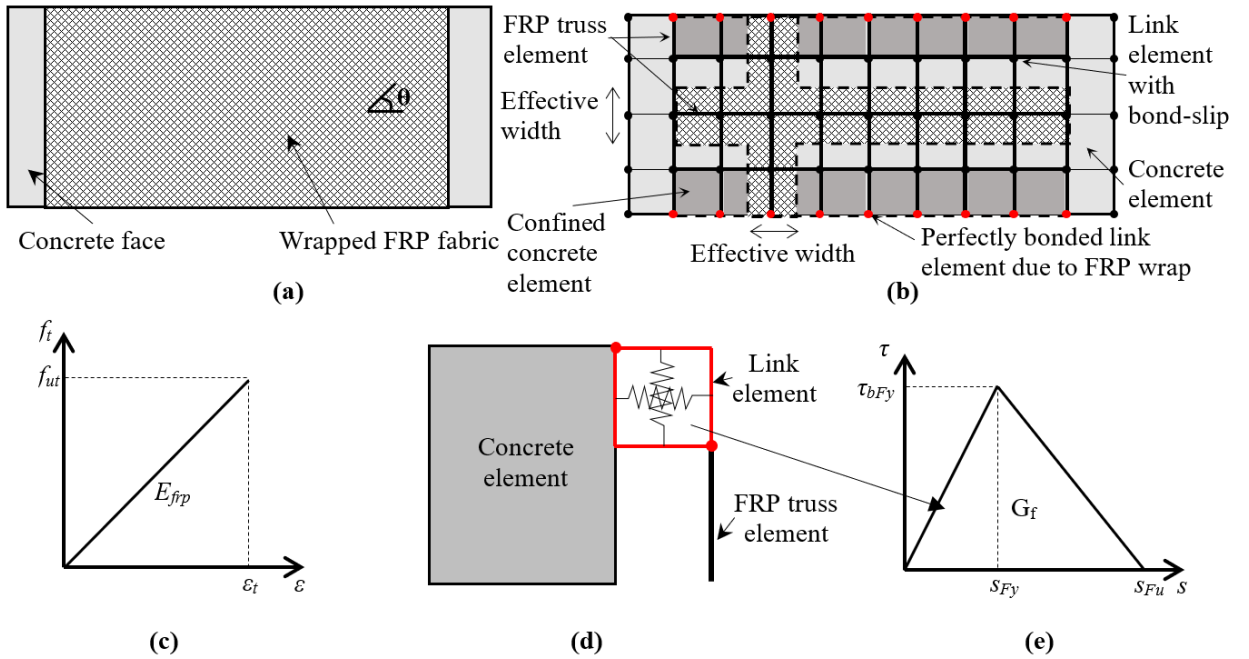

Figure 2 – (a) FRP fabric wrapped around the concrete element, (b) finite element modeling of FRP fabrics, (c) FRP constitutive model, (d) detail of link element between concrete and FRP fabric, and (e) bond-slip constitutive model.

System-Level Capacity Determination

To determine the structural capacity of the cap beam, a pushover analysis, where the finite element model is subjected to a monotonically increasing load up to the structural failure, is performed. Three loading procedures can be used, depending on the objective of the analysis:

The *first procedure* is used to assess the structural capacity of a non-existing cap beam, the pushover analysis is conducted from no load up to the maximum capacity of the structure, following the Strength I ultimate load combination as per the AASHTO[10] specifications of 1.25 x (Dead Load) + 1.75 x (Live Load). The *second procedure* is used when assessing the capacity of an existing cap beam, the pushover analysis is first conducted up to the Strength I ultimate load combination. Then, only the factored live load (LL) is continued to increase up to the structural failure. This loading procedure results in a more realistic assessment since the dead load (DL) that acts on the cap beam (i.e., the cap beam's own weight and bridge superstructure) is not expected to increase. The *third procedure* is used when analyzing the retrofitted structure, the FRP fabrics do not contribute to the original dead load that acts on the beam. Thus, a more realistic procedure is employed: the model is first loaded up to 100% factored dead load and no live load (i.e., 1.25DL + 0LL) with the retrofit elements turned off. From this point on, the retrofit elements are activated, and the dead load is kept constant while the factored live load (i.e., 1.75LL) is progressively increased up to the structural failure.

A global capacity factor method is preferred when calculating the design resistance of a member using NLFEA because nonlinear finite element constitutive models are highly sensitive to the material properties input values, particularly to the concrete strength (f'_c) and the reinforcement yield stress (f_y). Thus, the use of material resistance factors can artificially influence the response of the beam and may even change the failure mode. A full probabilistic analysis that considers the random distribution of the input parameters (i.e., material strengths) is considered the 'ultimate tool' for numerical performance assessments. However, such an approach would require several analyses (between 32 and 64[28]), which is not feasible for practical applications. In the proposed analysis methodology, the global capacity factor method proposed by Cervenka[28] is used. Cervenka studied different methods to calculate the design resistance of nonlinear analysis models and concluded that the estimate of the coefficient of variation method (ECOV), using only two analyses, yields results that are consistent with the full probabilistic method[28]. In the ECOV method, a global capacity factor (γ_G) is probabilistically obtained based on the coefficient of variation of the resistance (V_R) (see Equation 6), which is estimated based on the resistance of the structure using its characteristic (R_k) and mean (R_m) properties of materials, as defined by Equation 7. The design resistance is obtained from the mean resistance (R_m) and the calculated global capacity factor, as shown in Equation 8.

$$\gamma_G = \exp(\alpha_R \beta V_R) \tag{6}$$

$$V_R = \frac{1}{1.65} \ln\left(\frac{R_m}{R_k}\right) \tag{7}$$

$$R_d = \frac{R_m}{\gamma_G} \tag{8}$$

where α_R is the sensitivity factor for the resistance reliability, β is the reliability index, and R_d is the design resistance of the model. For a structural service life of 50 years, the recommended values of α_R and β are 0.8 and 3.8[29], respectively, for the ultimate limit state condition. For a service life of 75 years, α_R and β are 0.8 and 3.2, respectively. Similarly, AASHTO[10] recommends a reliability index of 3.5 for bridges. In this study, the reduction factor is calculated considering the service life of 50 years. As such, the global factor can be calculated using Equation 9.

$$\gamma_G = \exp(3.04 V_R) \tag{9}$$

The mean material properties of the reinforcing steel and concrete strengths can be calculated using Equations 10 and 11[30]. Since there is a lack of studies that indicate the mean tensile strength of FRP fabrics, this study used 25 technical sheets of different FRP fabrics manufacturer (15 of CFRP and 10 of GFRP) to obtain this factor for FRP fabrics. The factor for CFRP fabrics was calculated to be 1.18, which was slightly lower than the 1.20 factor for GFRP fabrics (see Equation 12). The mean bonding properties are inherently accounted for by the consideration of the mean concrete properties (see Equations 1-4).

$$f_{ym} = 1.1 f_{yk} \tag{10}$$

$$f_{cm} = 1.1\left(\frac{\gamma_s}{\gamma_c}\right) f_{ck} \quad (11)$$

$$f_{tm} = 1.18\sim1.20 f_{tk} \quad (12)$$

where f_{yk} and f_{ck} are the characteristic material properties for the reinforcing steel and concrete, respectively; γ_s and γ_c are the partial factors for materials for the ultimate limit states; and f_{tk} is the characteristic tensile strength of the FRP.

VERIFICATION OF THE PROPOSED MODELING APPROACH

The accuracy of the proposed material modeling approach was verified using two simply-supported beams experimentally retrofitted with CFRP fabrics: one with continuum CFRP U-wrap fabrics for shear strengthening[31] (see Figure 3a); and another with longitudinal CFRP fabrics for flexural strengthening anchored by U-wrapped fabrics[32] (see Figure 4a). The first specimen (originally referred to as SO3-4) was used to verify the bond-slip constitutive models (i.e., Equations 1-4) and the confinement effect of the fabrics (i.e., Equation 5). The second specimen (originally referenced as B70PW) was used to verify the bonding of the flexural FRP fabrics due to the provided anchorage fabrics.

The details of the experimental setup of each reinforced concrete beam are discussed elsewhere[31,32]. In short, the material properties experimentally reported and used in the NLFEA discussed herein were, for the SO3-4 beam[31]: concrete strength of 4 ksi (27.5 MPa), reinforcing steel modulus of elasticity, yield stress, and ultimate stress of 29000 ksi (200 GPa), 67 ksi (460 MPa), and 106 ksi (730 MPa), respectively, and CFRP modulus of elasticity and tensile strength of 33000 ksi (228 GPa) and 550 ksi (3790 MPa), respectively; and for the B70PW beam[32]: average concrete strength of 8 ksi (54 MPa), steel reinforcement modulus of elasticity and yielding strength of 29300 ksi (202 GPa) and 89 ksi (611 MPa), respectively, and CFRP modulus of elasticity and tensile strength of 31200 ksi (215 GPa) and 363 ksi (2500 MPa). Figures 3 and 4 presents the experimental setup, the created finite element model, and the beam deformations at failure for each specimen. Because U-wrap CFRP fabrics were used, only the nodes at the bottom edge of the beams were modeled as perfectly bonded. Similarly, the out-of-plane confinement reinforcement was modeled only for the concrete elements wrapped in the fabrics at the bottom edge of the beams (see Figures 3 and 4).

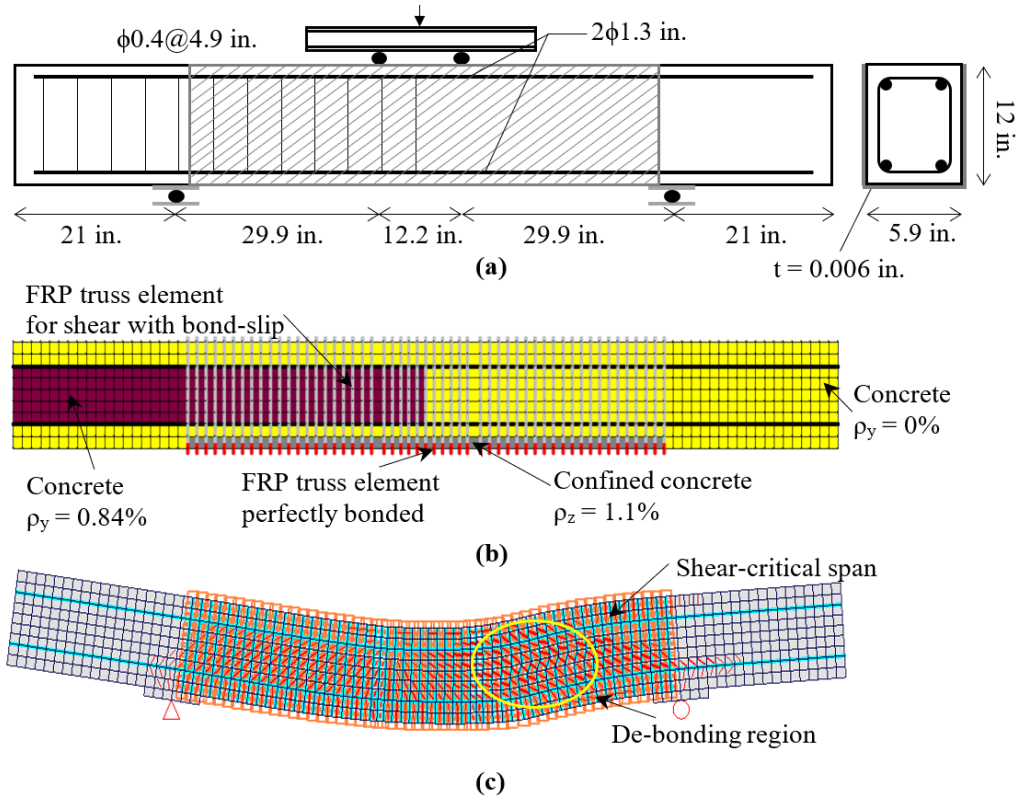

Figure 3 – (a) SO3-4 experimental setup, (b) finite element model, and (c) deflected shape at failure condition.

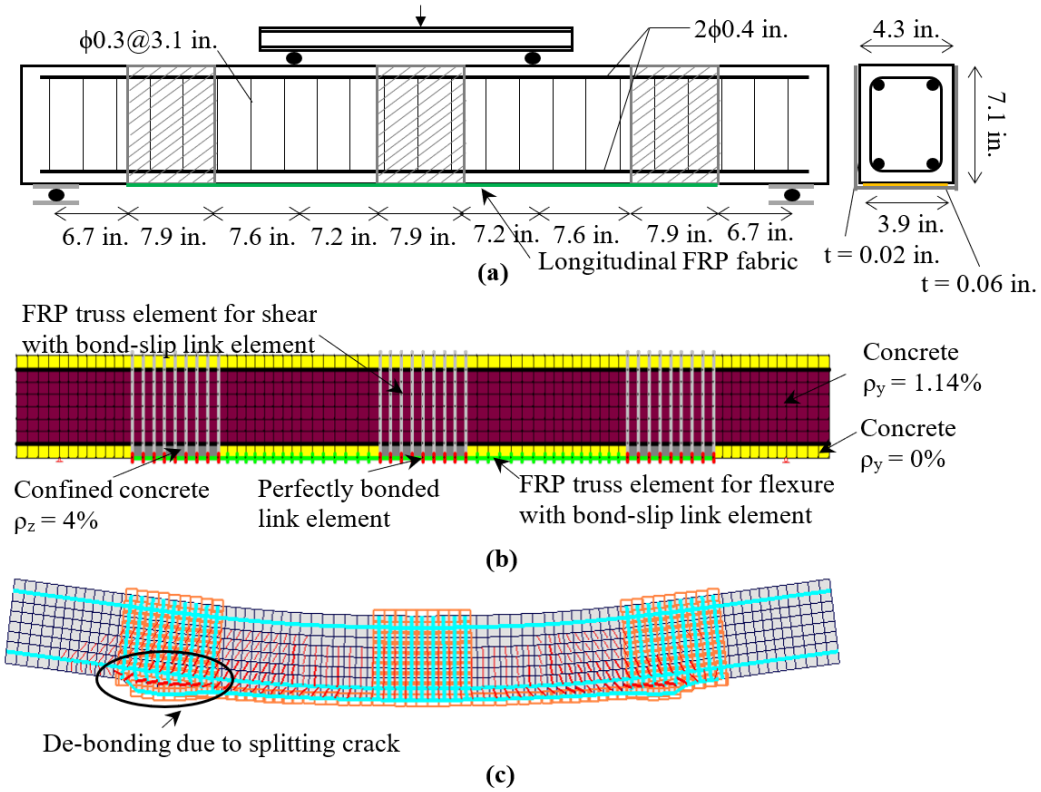

NOTE: 1 in. = 25.4 mm.

Figure 4 – (a) B70PW experimental setup, (b) finite element model, and (c) deflected shape at failure condition.

Figure 5 shows the load-deflection response experimentally obtained and numerically calculated by the created finite element model. The peak load, peak displacement and overall stiffness response of both beams were well captured by the finite element model. The calculated-to-experimental ratios (i.e., $1\text{-}P_{cal}/P_{exp}$) of the peak load capacity were -2.5% and 5.9% for the SO3-4 and the B70PW specimens, respectively. For the peak displacement, the calculated-to-experimental rations were 32.9% and 2.9% for the SO3-4 and the B70PW specimens, respectively. It is believed that the difference in peak displacement in the SO3-4 beam, despite its good overall response, was due to differences in the experimentally reported and actual material properties, which resulted in a slight stiffness deviation. The failure mode of the SO3-4 beam was experimentally reported to be the de-bonding of the CFRP U-wrap fabrics at a load of 65 kips (289 kN)[31]. The finite element model successfully calculated the failure mode as de-bonding of the CFRP fabrics starting at a load of 64 kips (285 kN) at the shear-critical span (see Figure 3c). The criteria used to identify de-bonding on the beams were based on the relative displacements between the CFRP fabrics and the concrete exceeding the slip at the maximum bond stress, after which bonding stresses decrease (i.e., as shown in Figure 2e). For the B70PW beam, the experimentally reported failure mode was a shear-tension failure with the initial flexural-shear cracks followed by the de-bonding of the flexural CFRP fabrics due to splitting cracks in the concrete[32]. The calculated failure mode of the beam captured the experimental response successfully as shown in Figure 4c, with splitting cracks at the bottom part of the beam that caused the de-bonding of the flexural CFRP reinforcement.

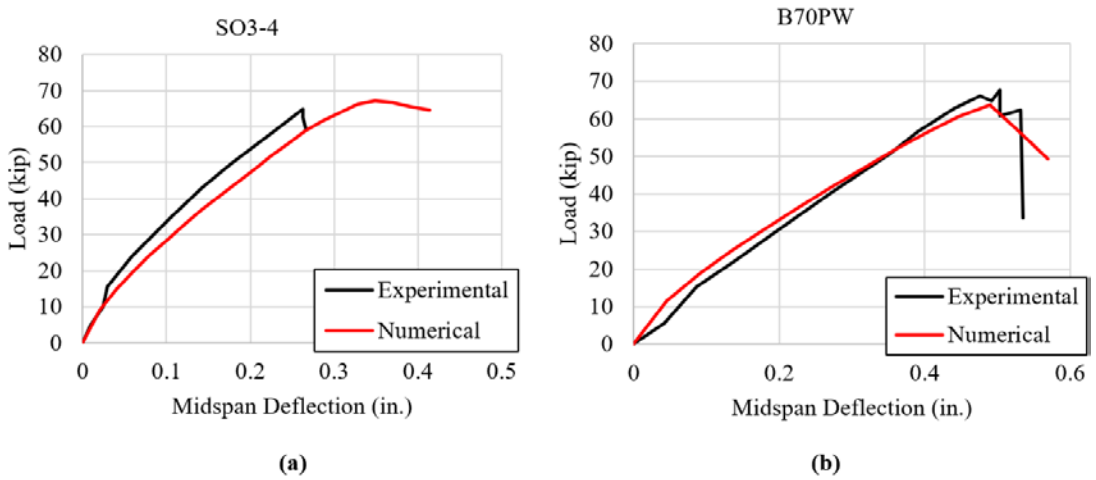

NOTE: 1 in. = 25.4 mm; 1 kip = 4.45 kN.

Figure 5 – (a) Cantilever and (b) inner span total load versus displacement response.

SYSTEM-LEVEL VERIFICATION OF THE NLFEA APPROACH

The proposed NLFEA approach was verified using a cap beam of an existing overpass structure (see Figure 6). Cross-sectional and a strut-and-tie model (STM) analyses calculated the cap beam to be overloaded. Thus, an NLFEA following the proposed modeling methodology was employed to calculate an accurate loading capacity of the cap beam.

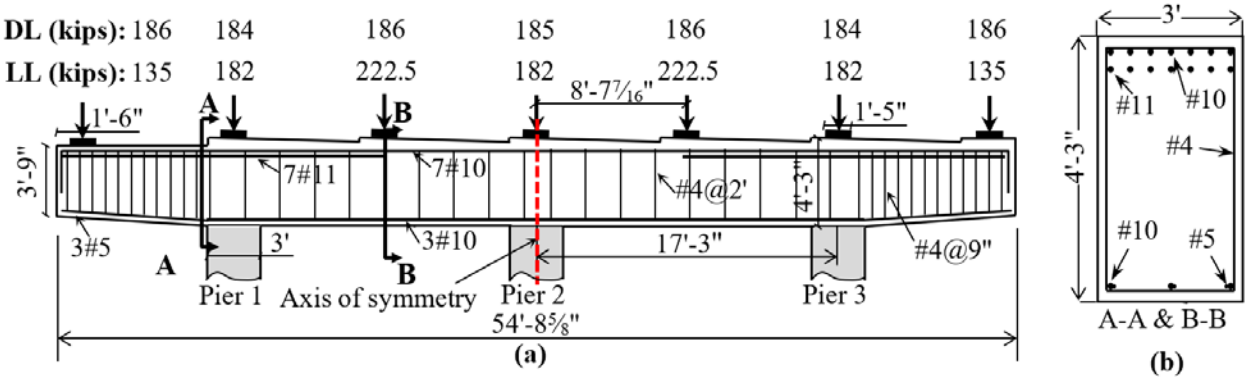

NOTE: 1 in. = 25.4 mm; 1 ft. = 0.305 m; 1 kip = 4.45 kN

Figure 6 – Cap beam examined: (a) elevation and (b) cross-section.

The finite element model was developed in VecTor2, as shown in Figure 7, with the cross-sectional dimensions, reinforcement layout, beam configuration, and unfactored loading condition shown in Figure 6. The concrete compressive strength and steel reinforcement yield stress were reported on the original design drawings as 4 ksi (27.6 MPa) and 40 ksi (275 MPa), respectively. The geometric symmetry of the beam allowed for a half-model of the cap beam, which significantly reduced the numerical model size and lowered the modeling efforts. The support conditions applied included rollers on the axis of symmetry and pins at the lowermost ends of the pier columns (not shown in Figure 7).

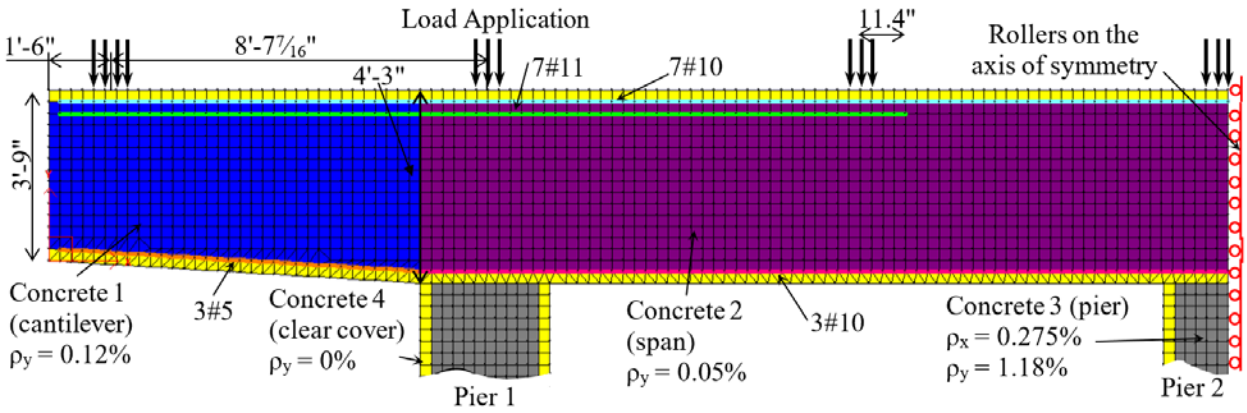

NOTE: 1 in. = 25.4 mm; 1 ft. = 0.305 m; 1 kip = 4.45 kN

Figure 7 – Finite element model developed for the NLFEA.

Three of the considered second-order models (see Table 1) were found to be particularly important for the cap beam examined: the concrete compression softening (i.e., the reduction in the uniaxial compressive strength and stiffness due to transverse tensile cracking), the concrete tension stiffening (i.e., the ability of cracked reinforced concrete to transmit tensile stresses across cracks), and the dowel action (i.e., the additional shear strength provided by the main reinforcing bars). The very low amounts of stirrup reinforcement present in the cap beam make it prone to shear cracking, which reduces the effectiveness of the concrete struts and, thus, requires the consideration of the 'concrete compression softening'. The cap beam is also prone to flexural cracking due to the lack of well-distributed layers of reinforcement, and thus its response is sensitive to the amount of tension transmitted across cracks, requiring the modeling of the 'concrete tension stiffening' effects. Finally, the low amount of stirrups reduce the shear capacity of the beam, such that the additional shear resistance due to the 'dowel action' becomes important.

The pushover loading procedure was performed for the assessment of existing cap beams (i.e., as the second proposed pushover loading method, see the "System-Level Capacity Determination" section). To obtain the design resistance of the cap beam, two analyses were performed: one with characteristic and one with mean properties of materials (as discussed in the "System-Level Capacity Determination" section). The mean values of the reinforcing steel and concrete strengths were calculated, using Equations 10 and 11, to be 44 ksi (275 MPa) and 3.32 ksi (22.9 MPa). For brevity, only the analysis results using the characteristic material properties are shown in this paper.

The characteristic pushover analysis calculated a maximum load capacity of 3447 kips (15333.2 kN), which represented approximately 90% of the ultimate load combination. At the failure condition (see Figure 8), an extensive shear and flexural cracking pattern were calculated at the cantilever span, which indicated the formation of the deep beam strut-action through shear cracks spanning from the point loads to the pier supports. The yielding of both top and bottom flexural reinforcement of the cap beam at the cantilever span caused the crushing of the concrete (i.e., high compressive strains) at the beam-column interface, contributing significantly to the propagation of the cracks (i.e., vertical cracks), resulting in a flexure-shear failure of the cap beam.

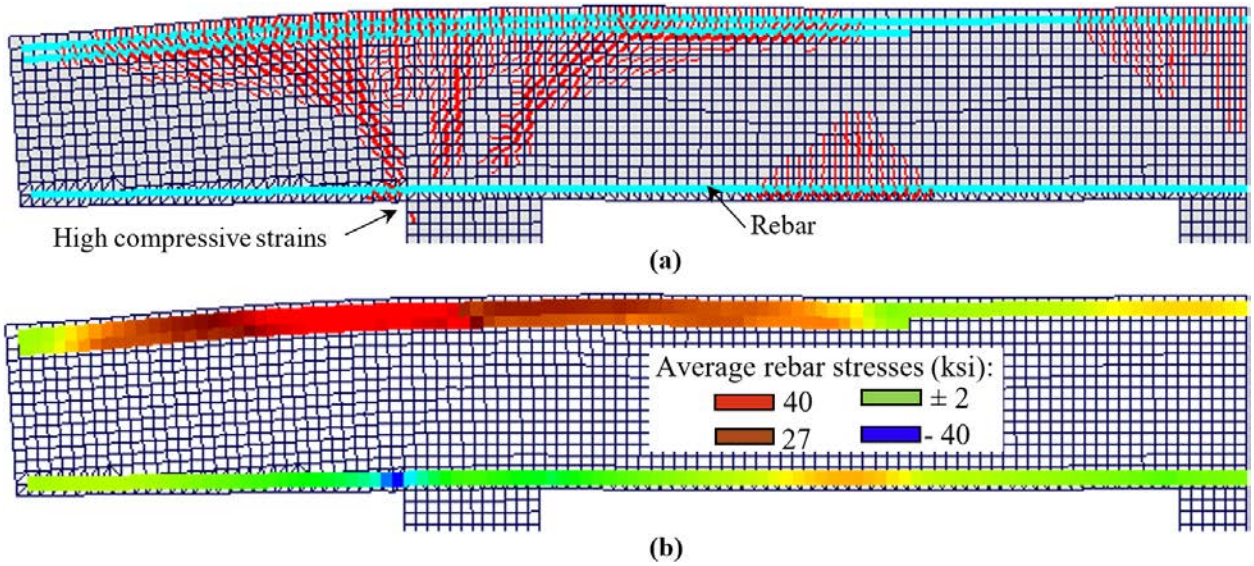

NOTE: 1 ksi = 6.9 MPa.

Figure 8 – Pushover analysis (a) crack pattern and (b) rebar stresses at failure loading condition (10 times actual deflection).

To obtain the system-level load capacity, the two performed pushover analyses were combined using Equations 7 and 9. The applied force versus displacement of the cantilever and inner span of the beams, for both analyses, are shown in Figure 9. The global capacity factor was calculated to be 1.10 and the design capacity of the cap beam was calculated, as per Equation 8, to be 3178 kips (14135 kN). Consequently, the un-retrofitted cap beam was found to be 17% overloaded. Thus, a retrofit study of the cap beam shall be performed to guarantee that the load resistance of the retrofitted cap beam surpasses its ultimate load demand.

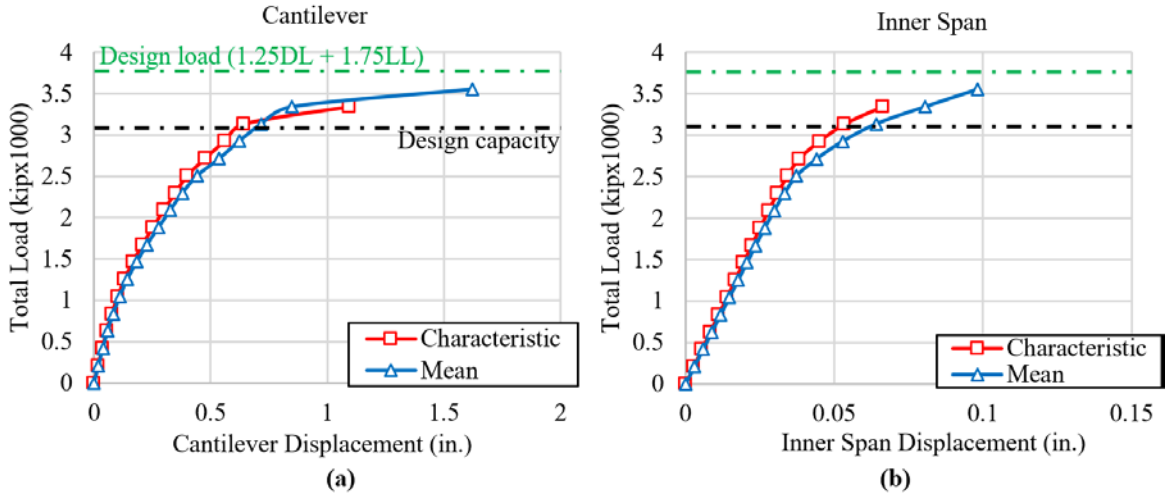

NOTE: 1 in. = 25.4 mm; 1 kip = 4.45 kN.

Figure 9 – (a) Cantilever and (b) inner span total load versus displacement response.

Retrofit of the cap beam using externally bonded FRP

A suitable FRP retrofit layout needs to be developed based on the failure mechanisms developed on the un-retrofitted structure. When studying an effective FRP retrofit layout, it is important to ensure that the new cap beam is capable not only to resist its un-retrofitted failure mechanisms but also to be able to resist new failure modes that can occur due to the redistribution of stresses caused by the added FRP fabrics. The critical failure modes for externally bonded FRP retrofitted structures are: concrete shear, concrete flexure, concrete compression (i.e., crushing), fabric de-bonding, and fabric rupture. A general FRP retrofit layout that covers the critical failure modes is proposed. As shown in Figure 10, this layout includes fabrics to increase shear capacity that are completely wrapped (i.e., black fabrics on

Figure 10) and U-wrapped (i.e., gray fabrics on Figure 10) around the concrete beam, and longitudinal fabrics that are bonded to the top and bottom of the beam to increase the flexural capacity (i.e., blue and green fabrics, respectively, on Figure 10). The completely wrapped FRP fabrics also provide effective anchorage to the longitudinal fabrics and confinement effects to the edges of the concrete beam. Consequently, besides its effective flexural and shear retrofit, this layout also improves the compressive capacity of the concrete (i.e., increasing its crushing resistance) and the bond-slip mechanism of the fabrics.

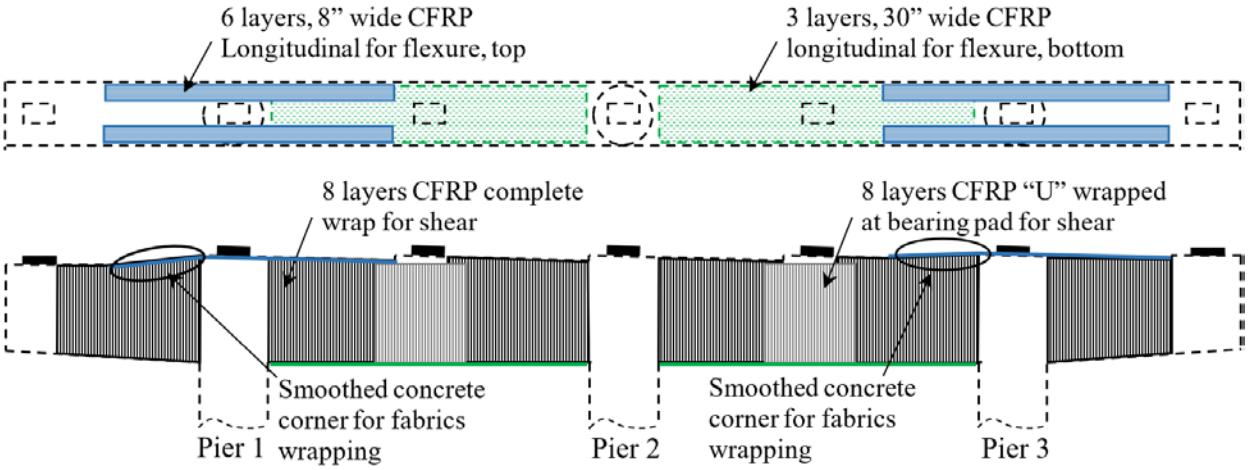

NOTE: 1 in. = 25.4 mm.

Figure 10 – FRP retrofit layout.

To determine the amount of FRP fabrics necessary to strengthen the beam (i.e., thickness and width of each fabric section of the FRP retrofit layout), different numerical models can be created (i.e., each one with a proposed amount of FRP fabrics) until the NLFEA calculates a safe structural condition under the ultimate loading condition. This process allows to effectively visualize the contribution and importance of each section of the FRP retrofit layout to the deficient structure. For conciseness, the fabric amounts for the final retrofit layout implemented on the studied cap beam is presented in Figure 10. The top longitudinal FRP fabrics were separated in two sections due to the locations of the bearing plates and some corners of the concrete beam were smoothed to help the fabrics application (see Figure 10). Similarly, the completely wrapped FRP fabrics were substituted by U-wrapped due to the presence of the bearing plates.

Once the externally bonded FRP layout was determined, it was implemented in the NLFEA model of the un-retrofitted structure (see Figure 11). The proposed FRP finite element material modeling approach was essential to ensure an accurate structural response and assessment of the additional capacity of the cap beam. In addition, the material modeling approach also modeled the critical failure modes (as discussed above): the concrete flexural and shear failure modes are covered by the employed concrete constitutive models; the compressive failure mode is covered by the concrete and FRP confinement effect models; the de-bonding is covered by the presented bond-slip relationship and the discussed perfect bonded regions; and the fabrics rupture is covered by the employed linear-elastic FRP material model. Thus, the determined effective FRP retrofit layout could be accurately incorporated in the NLFEA modeling approach, which makes it a suitable analysis procedure for accurate responses calculation.

The CFRP fabrics used had a modulus of elasticity, tensile strength, and thickness of 8200 ksi (56.5 GPa), 105 ksi (724 MPa), and 0.02 in. (0.51 mm), respectively. Using Equations 1-4, the calculated bond-slip properties of maximum bond stress, the slip at the maximum bond stress, and the slip at the ultimate bond stress were, 0.4 ksi (2.87 MPa), 9.83×10^{-4} in. (0.025 mm), and 5.20×10^{-3} in. (0.132 mm), respectively. Figure 11 shows the numerical model of the cap beam with the applied CFRP fabrics. Following the proposed FRP modeling approach, the CFRP fabrics were modeled with truss elements using the effective area of each truss and the bond-slip relationship. The wrapped fabrics (i.e., red truss elements in Figure 11) were perfectly bonded on the top and bottom edge of the concrete beam due to their complete wrapping (except over the bearing plate at the inner span). The bottom flexural fabrics were modeled as perfectly bonded due to the anchorage provided by the wrapped CFRP fabrics, and the top flexural fabrics were perfectly bonded at the anchorage regions. Out-of-plane confinement reinforcement was added to the concrete elements at the edges where the fabrics are wrapped.

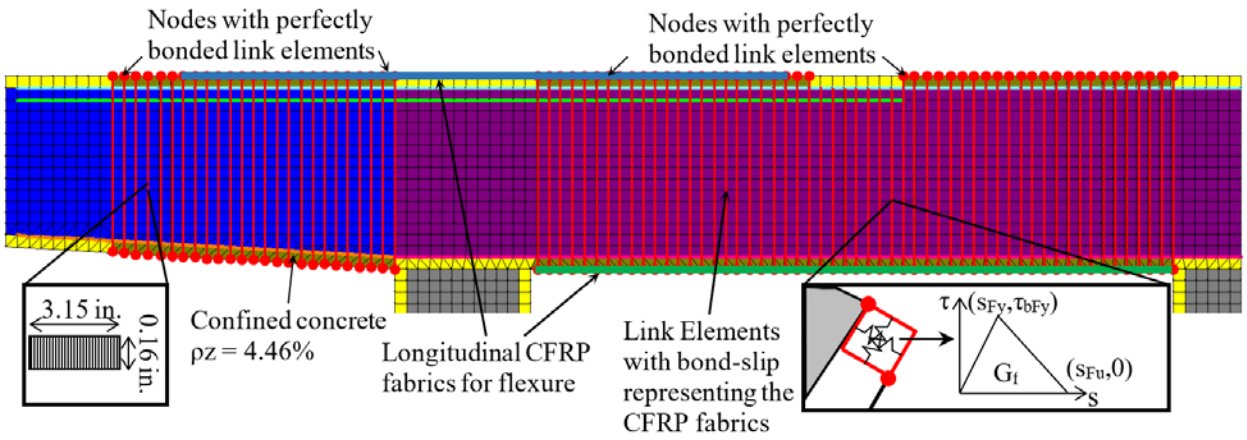

NOTE: 1 in. = 25.4 mm.

Figure 11 – Retrofitted finite element model.

For the system-level load capacity determination, the pushover loading procedure was performed following the method for the assessment of retrofitted structures (i.e., the third proposed pushover loading method, see the "System-Level Capacity Determination" section). The characteristic pushover analysis of the retrofitted structure showed an improvement in structural performance when compared to the same loading condition that caused the failure of the un-retrofitted cap beam (see Figure 12). Besides reducing the shear and flexural cracking condition at the cantilever and the inner span of the cap beam, the FRP retrofit layout also lowered the bottom reinforcement stress state and, in consequence, the concrete compressive strains at the cantilever-column interface.

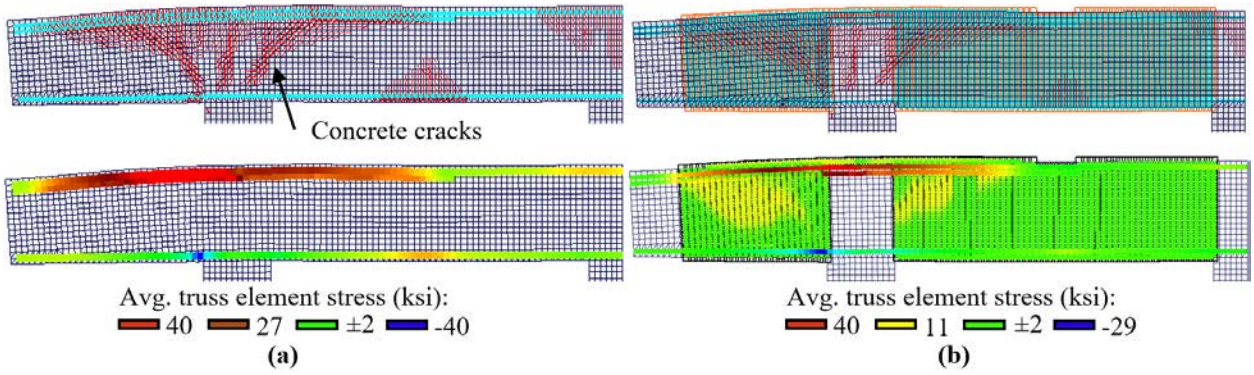

NOTE: 1 ksi = 6.9 MPa.

Figure 12 – (a) Un-retrofitted model at failure condition and (b) retrofitted model at same loading condition.

The characteristic pushover analysis of the retrofitted cap beam calculated a maximum capacity of 4050 kips (18018 kN). At the structural failure condition (exaggerated in Figure 13), extensive shear and flexural cracking patterns were observed. The high shear stresses on the cantilever span caused the FRP fabrics to de-bond following the main shear crack pattern (see Figure 13). The top and bottom reinforcing steel yielded and high compressive strains (i.e., concrete crushing) developed at the cantilever-column interface. The flexural capacity of the cantilever section relied mainly on the top longitudinal FRP fabrics, which, due to the high-stress demand, de-bonded through the split cracking of the adherent concrete, causing a flexure-shear failure of the cap beam.

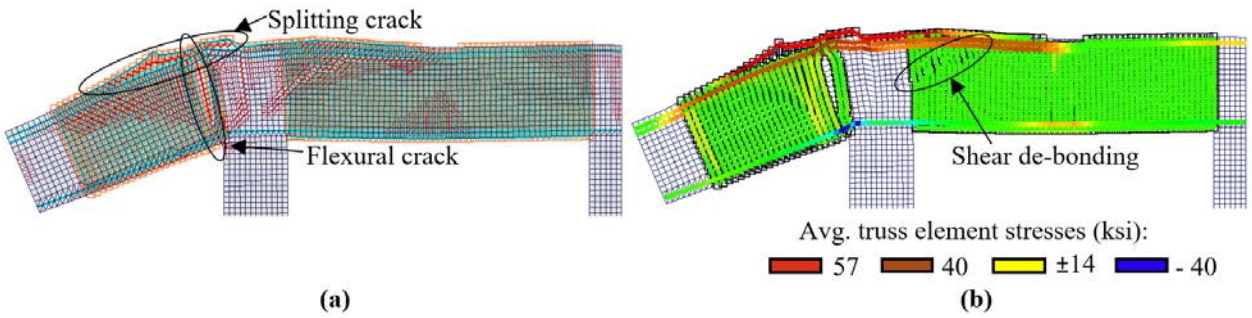

NOTE: 1 ksi = 6.9 MPa.

Figure 13 – (a) Retrofitted cap beam response and (b) rebar stresses at failure loading condition (20 times actual deflection).

Using Equations 7 and 9 with the results of the two analyses performed with the retrofitted finite element model (i.e., one with characteristic properties of material and one with mean properties of material), the calculated global capacity factor was 1.00 (both analyses calculated the same resistance) and the system-level load capacity of the retrofitted cap beam was determined to be 4050 kips (18018 kN). Figure 14 compares the characteristic pushover analysis responses of the un-retrofitted and retrofitted structure. In Figure 14, the last data point of each curve (i.e., the failure load and displacement) was selected for the loading condition at which the failure mechanisms that developed in each beam (and were described above) occurred. After this loading condition, the subsequent load stages of the numerical model were no longer representative of the real structural behavior (excessive displacements, zero-stresses, etc.) since failure mechanisms had already developed. The curves in Figure 14 do not present a strength peak (and subsequent loss of strength) due to the force-based nature of the numerical analysis performed. The calculated load capacity represented an increase of 27% in strength, when compared to the un-retrofitted cap beam (3178 kips or 14135 kN) and indicated an extra capacity of 6% over the ultimate loading condition. These results corroborate the benefits of the determined CFRP retrofit layout and the effectiveness of the modeling approach. As a result, the proposed methodology was successful in providing an effective FRP retrofit to the overloaded cap beam.

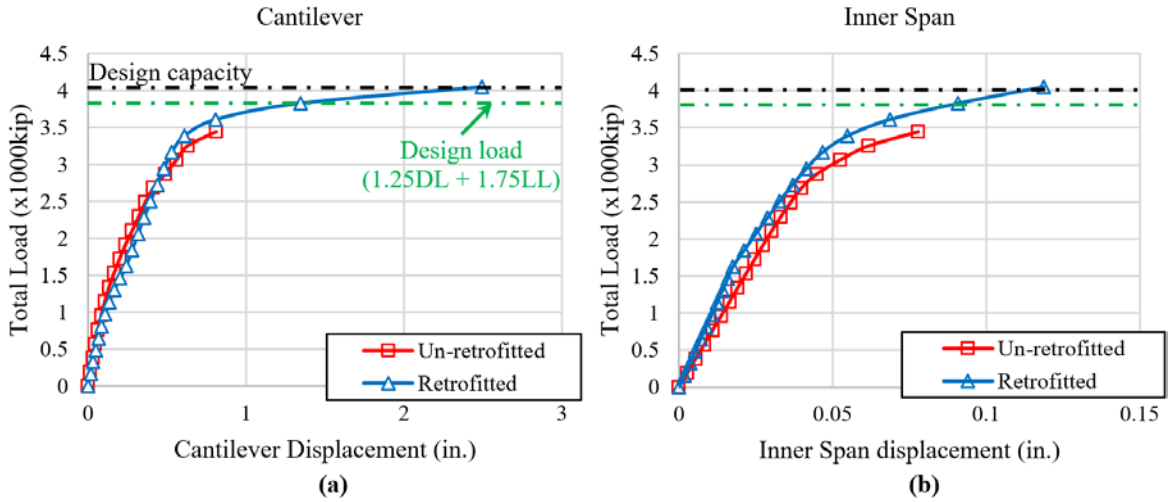

Figure 14 – (a) Cantilever and (b) inner span total load versus displacement response of the retrofitted model.

SUMMARY AND CONCLUSIONS

Deep bridge cap beams retrofitted with fiber reinforced polymers require special analysis methods in order to effectively account for behaviors that are characteristic of deep elements (such as the nonlinearity of the strain distribution and the effects of cracking on the stress distribution) and retrofit-related mechanisms (such as bond-slip relationships, confinement effects, and redistribution of stresses are not considered). Despite some equations given by available retrofit codes to calculate the extra capacity that FRP fabrics might produce on a general concrete element, no provisions account for the aforementioned behaviors that directly affect deep cap beams retrofitted with FRP fabrics. This study proposed an analysis methodology for deep cap beams retrofitted with externally bonded FRP fabrics. Details were given regarding the constitutive modeling of the critical behavior of materials, which were

verified using experimental results available in the literature. Finally, to exemplify the application of the proposed methodology, a real/large structure was analyzed, and an effective retrofit solution was calculated based on the calculated beam response. The results of this study support the following conclusions:

1. The proposed analysis methodology presented a comprehensive set of material behaviors and numerical modeling formulations that are essential for the analysis of deep cap beam elements. Three different loading approaches were defined to obtain a more accurate response of cap beams depending on the state of the bridge, i.e., non-existing bridge, existing bridge, retrofitted bridge. Finally, the proposed methodology presented a global capacity factor procedure based on probabilistic fundamentals for the determination of the design resistance of a cap beam.
2. The proposed methodology and its constitutive modeling approaches were successfully verified using two different experimental studies from the literature. The overall load-displacement deviation between the experimental results and the created methodology was calculated to be within 6%. In addition, the verification studies successfully verified the proposed FRP-concrete composite structural behavior, including the bond-slip constitutive model, concrete confinement effects caused by the fabric wrap, and the perfectly bonded conditions of longitudinal fabrics anchored by U-wrapped fabrics. As a result, the numerical model created using the proposed methodology was able to capture the experimentally observed failure modes.
3. An existing deep cap beam structure was analyzed to illustrate the benefits and in-depth information provided by the proposed methodology. The analyzed cap beam was calculated to be 17% overloaded considering the design ultimate load condition. The calculated response of the cap beam confirmed the deep beam action occurring on the beam through the calculated crack pattern, which also helped identify the most critical spans of the beam, the type of failure (i.e., flexure, shear, or flexure-shear), and critical effects that should be considered in the retrofit design.
4. The detailed damage pattern and failure mechanism calculated by the numerical model of the un-retrofitted cap beam were essential in the determination of an efficient distribution of the FRP fabric throughout the analyzed cap beam to capture the critical failure mechanisms. Such a design approach differs significantly from the use of code provisions, in which simplified equations are given to obtain the added capacity of the member due to the usage of FRP fabrics retrofit while neglecting important behaviors such as the deep beam effects, confinement effects, and bond-slip interaction.
5. The information obtained from the un-retrofitted numerical model was used to determine a CFRP retrofit layout on the overloaded cap beam. The proposed methodology was again used to create a retrofitted numerical model of the analyzed cap beam, which enabled an increase in the load carrying capacity of the cap beam by 27%, allowed it to be safe under its ultimate loading condition, and developed an additional 6% extra capacity.
6. The general FRP retrofit layout configuration used in the studied cap beam (i.e., position and distribution of fabrics, but not their quantities) could be applied for a general cap beam as long as its failure conditions follow the trend observed in the structure analyzed in this paper. The number of fabric's layers and material properties on each section of the FRP retrofit layout can be studied to result in the desired structural performance.

ACKNOWLEDGMENTS

The authors would like to thank the Ohio Department of Transportation for providing the structural design drawings and the contributions of Dr. Douglas K. Nims and Mr. John R. Morganstern for extracting the main structural details and participating in several meetings to discuss the various aspects of the bridge.

REFERENCES

[1] American Concrete Institute, "*Guide for the Design and Construction of Structural Concrete Reinforced with FRP Bars (ACI 440.1R-15),"* American Concrete Institute (ACI), Farmington Hills, MI, 2015, 88 pp.

[2] Canadian Standards Association / National Standard of Canada, "*Canadian Highway Bridge Design Code (CAN/CSA S6-14),"* 11th ed., CSA Group, Mississauga, Ontario, Canada, 2014, 894 pp.

[3] American Concrete Institute, "*Building Code Requirements for Structural Concrete and Commentary (ACI 318-19),"* American Concrete Institute, Farmington Hills, MI, 2019, 624 pp.

[4] Canadian Standards Association, "*Design of Concrete Structures (CSA A23.3-14),*" 6th ed., CSA Group, Mississauga, Ontario, Canada, 2014, 290 pp.

[5] Guner, S.; Vecchio, F. J., "Pushover Analysis of Shear-Critical Frames: Formulation," *ACI Structural Journal,* V. 107, No. 1, 2010, 63-71 pp., http://www.utoledo.edu/engineering/faculty/serhan-guner/docs/JP1-Guner and Vecchio.pdf.

[6] Guner, S.; Vecchio, F. J., "Pushover Analysis of Shear-Critical Frames: Verification and Application," *ACI Structural Journal,* V. 107, No. 1, 2010, 72-81 pp., http://www.utoledo.edu/engineering/faculty/serhan-guner/docs/JP2_Guner_Vecchio_2010b.pdf.

[7] Wong, P. S.; Vecchio, F. J.; Trommels, H., *"Vector2 & Formworks User's Manual,"* 2nd ed., 318 pp., http://www.vectoranalysisgroup.com/user_manuals/manual1.pdf.
[8] Vecchio, F. J., "Disturbed Stress Field Model for Reinforced Concrete: Formulation," *Journal of Structural Engineering*, V. September, 2000, 1070-1077 pp., http://www.vectoranalysisgroup.com/journal_publications/jp34.pdf.
[9] Vecchio, F. J.; Collins, M. P., "The Modified Compression-Field Theory for Reinforced Concrete Elements Subjected to Shear," *ACI Journal*, V. 83, No. 2, 1986, 219-231 pp., http://www.vectoranalysisgroup.com/journal_publications/jp2.pdf.
[10] American Association of State Highway and Transportation Officials. "*AASHTO LRFD Bridge Design Specifications,"* 4th ed., American Association of State Highway and Transportation Officials, Washington, DC, 2017, 566 pp.
[11] Hognestad, E., "A Study of Combined Bending and Axial Load in Reinforced Concrete Members," *Bulletin Series No 399*, 1951, 128 pp., https://www.ideals.illinois.edu/handle/2142/4360%0Ahttp://hdl.handle.net/2142/4360.
[12] Coulomb, C. A., "Essai Sur Une Application des Regles de Maximis et Minimis a Quelques Problemes de Statique Relatifs a l'Architecture (Essay on Maximums and Minimums of Rules to Some Static Problems Relating to Architecture)," *Memoires De La Mathematique Et De Physique*, V. 7, 1973, 343–387 pp.
[13] Bunni, N. G.; Scott, B.; Park, R.; Priestley, M., "Stress-Strain Behavior of Concrete Confined by Overlapping Hoops at Low and High Strain Rates," *ACI Journal*, V. 79, No. 6, 1982, 496-498 pp.
[14] Vecchio, F. J., "Analysis of Shear-Critical Reinforced Concrete Beams," *ACI Structural Journal*, V. 97, No. 1, 2000, 102-110 pp.
[15] Vecchio, F. J., "Finite Element Modeling of Concrete Expansion and Confinement," *Journal of Structural Engineering*, V. 118, No. 9, 1992, 2390-2406 pp.
[16] Bentz, E. C., "Explaining the Riddle of Tension Stiffening Models for Shear Panel Experiments," *Journal of Structural Engineering*, V.131, No. 9, 2005, 1422-1425 pp., http://ascelibrary.org/doi/10.1061/%28ASCE%290733-9445%282005%29131%3A9%281422%29.
[17] Walraven, J. C.; Reinhardt, H. W., "Theory and Experiments on the Mechanical Behaviour of Cracks in Plain and Reinforced Concrete Subjected to Shear Loading," *Heron*, V. 26, No. 1A, 1981, https://repository.tudelft.nl/islandora/object/uuid:3d68bd1a-465d-4590-b33c-7ede99bbc251/datastream/OBJ/download.
[18] Seckin, M., "Hysteretic Behavior of Cast-In-Place Exterior Beam-Column-Slab Assemblies," *Ph.D. Thesis*, University of Toronto, Toronto, Canada, 1982.
[19] Kupfer, H.; Hilsdorf, H., "Behavior of Concrete Under Biaxial Stresses," *ACI Journal*, V. 66, No. 8, 1969, 656-666 pp., http://www.academia.edu/download/33736623/kupfer.pdf.
[20] Richart, F.; Brandtzaeg, A.; Brown, R. L., "A Study of the Failure of Concrete under Combined Compressive Stresses," *University of Illinois Bulletin*. V. 26, Bullet(12), 1928, 104 pp., http://www.academia.edu/download/33736623/kupfer.pdf.
[21] He, X. G.; Kwan, A. K. H., "Modeling Dowel Action of Reinforcement Bars for Finite Element Analysis of Concrete Structures," *Computers and Structures*, V. 79, No. 6, 2001, 595-604 pp.
[22] Dhakal, R. P; Maekawa, K., "Modeling for Postyield Buckling of Reinforcement," *Journal of Structural Engineering*, V. 128, No. 9, 2002, 1139-1147 pp., http://ascelibrary.org/doi/10.1061/%28ASCE%290733-9445%282002%29128%3A9%281139%29.
[23] Dhakal, R. P.; Maekawa, K., "Reinforcement Stability and Fracture of Cover Concrete in Reinforced Concrete Members," *Journal of Structural Engineering*, V. 128, No. 10, 2002, 1253-1262 pp.
[24] Grelle, S. V; Sneed, L .H., "Review of Anchorage Systems for Externally Bonded FRP Laminates," *International Journal of Concrete Structures and Materials*, V. 7, No. 1, 2013, 17-33 pp.
[25] Sato, Y.; Vecchio, F. J., "Tension Stiffening and Crack Formation in Reinforced Concrete Members with Fiber-Reinforced Polymer Sheets," *Journal of Structural Engineering*, V. 129, No. 6, 2003, 717-724 pp.
[26] Wong, R. S.; Vecchio, F. J., "Towards Modeling of Reinforced Concrete Members with Externally Bonded Fiber-Reinforced Polymer Composites," *ACI Structural Journal*, V. 100, No. 6, 2003, 47-55 pp., http://www.vectoranalysisgroup.com/journal_publications/jp45.pdf.
[27] Ceroni, F.; Pecce, M.; Matthys, S.; Taerwe, L., "Debonding Strength and Anchorage Devices for Reinforced Concrete Elements Strengthened with FRP Sheets," *Composites Part B: Engineering*, V. 39, No. 3, 2008, 429-441 pp., doi:10.1016/j.compositesb.2007.05.002
[28] Cervenka, V., "Global Safety Format for Nonlinear Calculation of Reinforced Concrete," *Beton- und Stahlbetonbau*, V. 103, No. S1, 2008, 37-42 pp., http://doi.wiley.com/10.1002/best.200810117.

[29] Sangiorno, F., “Safety Format for Non-linear Analysis of RC Structures Subjected to Multiple Failure Modes,” *Ph.D. Thesis*, KTH Royal Institute of Technology, Stockholm, Sweden. 2015, 45pp.
[30] European Committee for Standardization. *Eurocode 2 - Design of Concrete Structures - Concrete Bridges - Design and Detailing Rules (EN 1992-2:2005)*. European Committee for Standardization (CEN), 2005, 95 pp.
[31] Khalifa, A.; Nanni, A., “Rehabilitation of Rectangular Supported RC Beams with Deficiencies Using CFRP Composites,” *Construction and Building Materials*, V. 16, No. 3, 2002, 135-146 pp.
[32] Al-Tamimi, A. K.; Hawileh, R.; Abdalla, J.; Rasheed, H. A., “Effects of Ratio of CFRP Plate Length to Shear Span and End Anchorage on Flexural Behavior of SCC RC Beams,” *Journal of Composites for Construction*, V. 15, No. 6, 2011, 908-919 pp.